BULLETIN OF THE POLISH ACADEMY OF SCIENCES
TECHNICAL SCIENCES, Vol. 74(2), 2026, Article number: e157564
DOI: 10.24425/bpasts.2026.157564

Experimental study on ammonolysis process of copper(II) nitrate and copper oxide-copper nitride transformations

Robert SZCZĘSNY*, Katarzyna BOGDAŃSKA, and Marek WIŚNIEWSKI

Faculty of Chemistry, Nicolaus Copernicus University in Toruń, Gagarina 7, 87-100 Toruń, Poland

Abstract. There has been renewed interest in copper nitride (Cu_3N). New chemical methods have been developed to synthesize this compound in the last ten years. Although these approaches are based on the precipitation reaction exploiting different nitriding agents, an interesting issue is still the applicability of the gas (NH_3) – solid ammonolysis process towards various precursors and the analysis of the course of this reaction. The nitridation processes of the copper(II) nitrate and the subsequent formation of copper oxide-copper nitride were analyzed in this study. The mentioned phase transformations were monitored *in situ* by infrared spectroscopy. Moreover, X-ray powder diffraction (XRD) and scanning electron microscopy (SEM) were employed for morphology and phase composition analysis. The results indicate that $Cu(NO_3)_2$ can serve as an effective direct Cu_3N precursor. This ammonolysis reaction proceeded through the formation of copper oxides. Additionally, ammonolysis-oxidation tests between CuO and Cu_3N indicate the full reversibility of these processes.

Keywords: copper nitride; copper oxide; ammonolysis reaction; gaseous ammonia; infrared spectroscopy.

1. INTRODUCTION

Copper nitride (Cu_3N) is a metastable semiconductor that has been the subject of intensive research in recent years due to its unique properties and potential applications across various technological fields [1–3]. Its non-toxic nature and the ability to be synthesized using environmentally friendly methods are noteworthy [1, 2]. Its exceptional electrical and optical properties make it suitable for applications in photovoltaics [4–6], optical storage [7], spintronic systems [8], or as an electrode material for batteries [9, 10]. Recently, Cu_3N has also been studied for various electrocatalysis applications, including electrochemical CO_2 reduction reaction (CO_2RR) [11–13]. For many years, Cu_3N thin layers fabricated by physical deposition methods, such as reactive radio-frequency (RF) magnetron sputtering [14] and pulsed laser deposition (PLD) [3, 15], have been the main research area concerning this semiconductor. However, the first synthesis of copper nitride was conducted using chemical methods. The powders of Cu_3N were synthesized by Juza and Hahn [16] in 1938 by thermal treatment of a copper(II) fluoride precursor under gaseous ammonia. In further studies, new chemical methods were developed, based mainly on sources other than $NH_{3(g)}$ nitridation. In 1990, Zachwieja and Jacobs proposed the pathway realized *via* the direct thermal decomposition of $[Cu(NH_3)_x]NO_3$ salt [17]. Choi and Gillan synthesized nanocrystalline Cu_3N from an unstable copper azide in a non-aqueous solvothermal reaction [18]. In the following years, most reported approaches to Cu_3N nanocrystal chemical synthesis were based on $Cu(NO_3)_2$ decomposition in a solution containing long-chain amines acting simultaneously as solvents, capping agents, and nitrogen sources [19, 20]. Other alternative nitrogen sources were also reported [21–23]. However, publications presenting a "classical" nitridation source – gaseous ammonia – have also appeared in recent years [24–28]. These include our studies where we used copper(II) oxide or hydroxide as precursors, heated in an ammonia atmosphere. The presented results extend our previous work on copper nitride fabrication [2, 24–27] and intend to demonstrate that the "classical" nitridation method is still worth studying as an effective solution for obtaining diverse morphological powders and nanostructures. We present research on the ammonolysis monitored using *in situ* infrared spectroscopy, X-ray powder diffraction (XRD), and scanning electron microscopy (SEM). We chose the reaction of ammonia gas with copper(II) nitrate as a precursor, which was not previously studied in detail in the gas-solid synthesis of unsupported Cu_3N. We believe that using this salt could be a convenient alternative in some circumstances. This soluble salt can be easily deposited by impregnation on a specific, porous base material, and then directly heated under ammonia, resulting in copper nitride loaded onto the chosen support. Moreover, we present studies on the subsequent transformation of copper nitride – copper(II) oxide crystal phases, focusing on possible changes in the crystallinity, size, and powder morphology induced by heating processes in an ammonia and air atmosphere.

*e-mail: roszcz@umk.pl

Manuscript submitted 2025-03-30, revised 2025-12-14, initially accepted for publication 2026-01-01, published in March 2026.

2. MATERIALS AND METHODS

2.1. Chemicals and $Cu(NO_3)_2{\cdot}3H_2O$/Si material fabrication

$Cu(NO_3)_2 \cdot 3H_2O$ and Gaseous NH_3 (POCh, Poland) were of analytical grade (99.999%) and used as purchased. Copper salt was embedded on a dry and cleaned (hot 2-propanol rinsing) Si wafer (20 μm thick) *via* the dip-coating method (2 mm/min).

2.2. Methods

The processes were performed in custom-designed equipment that allows the sample to be placed and thermally treated at a given temperature in a selected gas atmosphere or in a vacuum, while simultaneously monitoring chemical changes for 60 minutes, using infrared spectroscopy in transmittance mode [29–33]. Experiments were performed up to 320°C under different atmospheres and pressures: vacuum ($p = 10^{-3}$ Torr), ammonia NH_3 ($p = 10$ Torr and $p = 300$ Torr), and air ($p = 760$ Torr). The target annealing temperature of 320°C was selected for both types of experiments following the literature [24–27].

The IR spectra were collected *in situ* using a Mattson-Genesis II spectrometer. Measurements were performed of the heterogeneous reactions of material films loaded on Si(100) and exposed to an NH_3, oxygen atmosphere, or vacuum. Note that the spectra were collected in the transmission mode, and the spectrum of a particular gaseous phase was the background. To remove any SiO_2 traces from the Si(100) surface, the wafers were immersed in the HF bath (2 h at 25°C) and washed in deionized water several times in an ultrasonics bath (1 h). The copper(II) nitrate sample was applied to separate plates for the ammonolysis reactions conducted under different conditions (vacuum or ammonia gas atmosphere). In experiments concerning reversible oxide-nitride transformations, the tests were set to use the same sample in successive heating cycles. Sections 3.1–3.3 contain further descriptions and explanations.

The powdered products were identified by X-ray diffraction (XRD) using an X'Pert Pro $\theta - 2\theta$ diffractometer (PANalytical) with CuKα radiation. Scanning electron microscopy (SEM) studies were performed with a Quanta 3D FEG (FEI) (EHT = 30 kV) instrument. Open-source software ImageJ was applied for SEM image analysis.

3. RESULTS

3.1. Heating of copper(II) nitrate under vacuum

The first experiment was conducted under a vacuum. Copper(II) nitrate was dripped onto the substrate, dried, and mounted under the equipment, ensuring the selected atmosphere, temperature, and the possibility of *in situ* recording of the IR spectrum. The results are presented in Fig. 1. The spectra registered between 25 and 150°C indicate that the dehydration process of copper salt took place in this range. The broad peak with a maximum of *ca.* 3330 cm^{-1} was initially observed at room temperature. Copper(II) nitrate is hygroscopic, and this band can be related to the presence of the hydrated form of this compound. As the temperature increases, the intensity of this band decreases. At 100°C, the emergence of a band at approximately 3550 cm^{-1} can be noticed. According to the literature, it can be assumed that basic copper nitrate $Cu_2(NO_3)(OH)_3$ is formed at this temperature [34–36]. Above 200°C, all bands derived from nitrate nearly disappeared, whereas bands derived from copper(II) oxide emerged (Fig. 1e–h). The formation of CuO in low-pressure conditions has also been reported by other authors [36, 37].

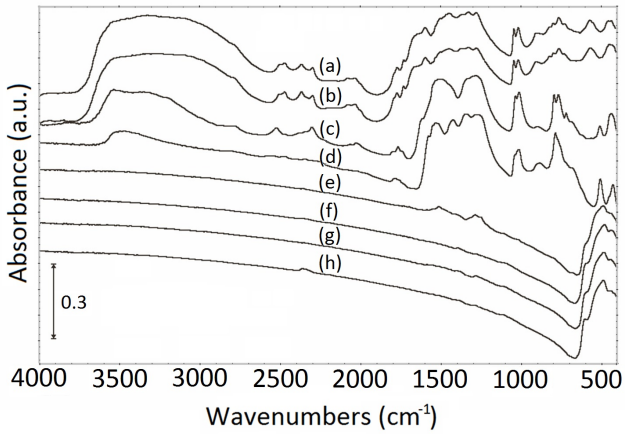

Fig. 1. IR spectra of $Cu(NO_3)_2$ treated under vacuum at (a) 25°C, (b) 50°C, (c) 100°C, (d) 150°C, (e) 200°C, (f) 250°C, (g) 300°C, (h) 320°C

3.2. Ammonolysis reactions of copper(II) nitrate

The ammonolysis process of copper(II) nitrate monitored by infrared spectroscopy was conducted at two ammonia levels, as shown in Fig. 2. In the first case, the copper precursor was heated under a 10 Torr pressure of gaseous ammonia (Fig. 2A), whereas in the second stage, the pressure of ammonia introduced into the system was increased to 300 Torr (Fig. 2B). Before starting the heating, the air was evacuated, and the gaseous NH_3 was introduced into the vessel with the deposited copper(II) salt. At this point, the IR spectra showed peaks at 1420, ~ 1340, and 1040 cm^{-1}, which can be assigned to the normal modes of

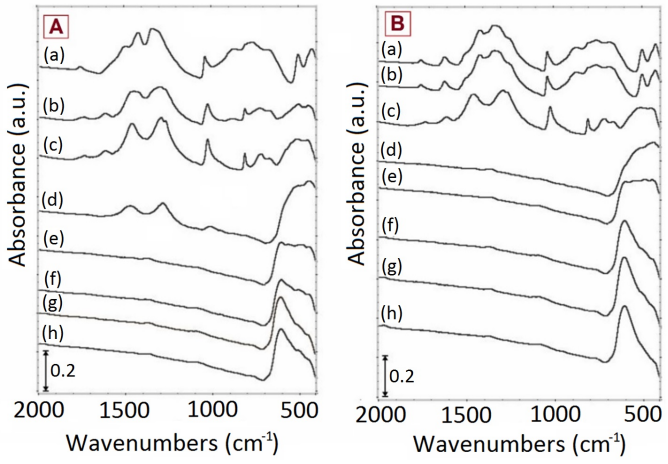

Fig. 2. IR spectra of $Cu(NO_3)_2$ treated under: (A) 10 Torr NH_3 at (a) 25°C, (b) 50°C, (c) 100°C, (d) 150°C, (e) 200°C, (f) 250°C, (g) 300°C, (h) 320°C; (B) 300 Torr NH_3 at (a) 25°C, (b) 50°C, (c) 100°C, (d) 150°C, (e) 200°C, (f) 250°C, (g) 300°C, (h) 320°C

asymmetric stretching (ν_3) and stretching (ν_1) of nitrate ions in the tetraamminecopper(II) complex, respectively [35, 38]. A rise in temperature under an ammonia atmosphere to 150°C (Figs. 2A(d) and B(d)) results in significant changes in the intensity of the above-mentioned peaks. However, vibrations derived from nitrate nearly disappeared in the case of a spectrum for a 300 Torr pressure of NH_3. For a 10 Torr ammonia pressure, such an effect is visible at 200°C. The disappearance of the bands above 700 cm^{-1} correlates with the formation of intensive signals between 400–600 cm^{-1}, which can be associated with frequencies characteristic of copper(II) oxide [39,40]. However, according to the literature, the coexistence of CuO and Cu_2O phases can also be assumed [41–43]. In the case of a sample heated under a 10 Torr pressure of ammonia, a strong absorption band above 600 cm^{-1} appeared at the highest temperatures (Fig. 2A(g–h)). This feature may indicate copper(I) nitride and copper(I) oxide phase mixture after annealing [44,45]. The process is more effective for experiments conducted with a 300 Torr pressure of ammonia (Fig. 2B), and the final sharp peak after heating the sample at 320°C for 60 minutes can be ascribed to the vibration of Cu-N [46].

The conditions mentioned were applied for the tests presented in the next paragraph and were selected since they enable the effective conversion of the Cu-O bond into the Cu-N bond.

3.3. Copper oxide – copper nitride transformation

This paragraph concerns the subsequent conversion between copper(II) oxide – copper nitride phases. The experiments were conducted based on our previous studies [24, 25, 27]. We noticed that heating in gaseous ammonia induces subtle changes in the crystallites of the annealed powders/nanostructures. For this reason, we analyze how heating affects the morphology during copper(II) oxide transition to copper nitride and *vice versa*, as this knowledge may be useful when employing Cu_3N as a reversible sensor or catalyst, given that the nitride oxidizes to copper(II) oxide under ambient conditions. The powders obtained under a 300 Torr pressure of ammonia and by heating under air at 320°C were analyzed by XRD and SEM. Powder X-ray and IR spectroscopy analysis clearly showed only copper nitride and copper(II) formation (Figs. 3A, 3B). The crystallite size and microstrain were calculated from the X-ray diffraction (XRD) data obtained for the four samples. The changes in the successive stages of the transformation are shown in Fig. 4. The calculations were performed using the Scherrer formula for the crystallite size and the theoretical formula for microstrain based on the full width at half maximum (FWHM) and the integral breadth (IB) methods for two peaks from each diffractogram [47]. The selection of individual peaks was governed by their intensity and matching with copper oxide and copper nitride reference patterns. The size of the copper oxide (**CuO_1**) crystallites ranges from 13.72 to 17.85 nm for the FWHM method and from 12.34 to 15.82 nm for the IB method. After annealing in ammonia and then in air, these values did not change significantly for **CuO_2**. A similar trend is apparent for the lattice strain values. However, changes occur in the case of copper nitride. For **Cu_3N_1**, the crystallite size varies between 14.42 and 21.12 nm and 12.81 and 18.78 nm for the FWHM and IB methods, respectively. As a result of annealing in the obtained **Cu_3N_2**, the crystallite size decreased to 13.80–17.07 nm for FWHM and 12.44–15.79 nm for IB. Microstrains exhibit the opposite trend, showing a significant increase in strain. Comparing the crystallite size and microstrain values determined by the two methods of FWHM and IB, it was noted that the crystallite size calculated for FWHM is larger than that determined by the IB method. Strains display the opposite trend. The changes presented in Fig. 4 may arise from various factors, including cooling/heating rate, annealing temperature, and time, and making their origin difficult to interpret unequivocally [48, 49]. Studies describe the effect of air annealing, showing that the size of crystallites heated in air increases with temperature. Simultaneously, the decrease in microstrain values is observed [50–52]. The increase of crystallite size is also noticed for the ammonolysis process [53, 54]. Most studies focus on the influence of temperature under both

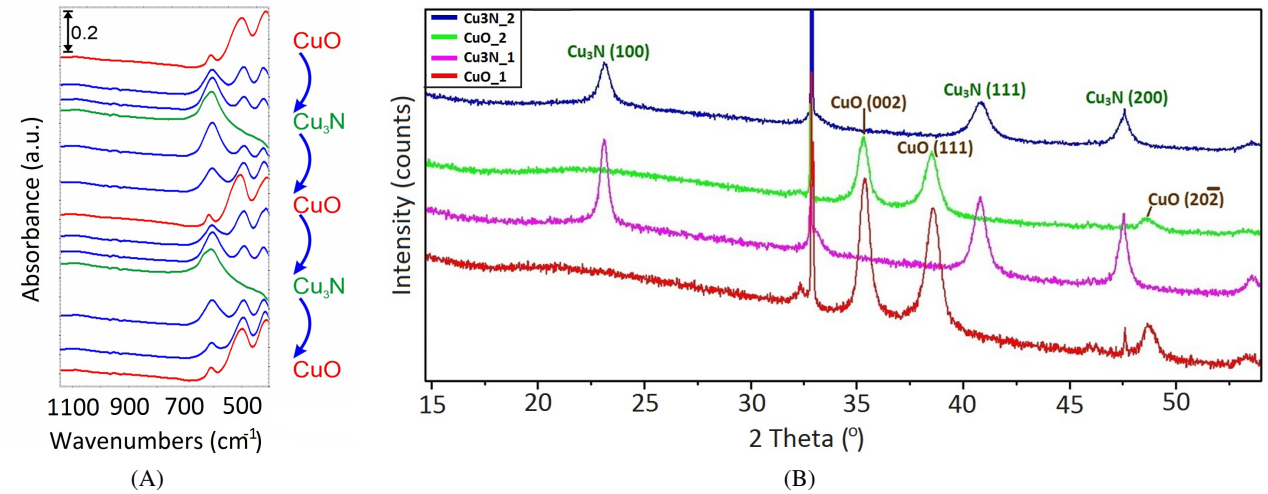

Fig. 3. (A) FTIR spectra of cycles showing the CuO to Cu_3N reversibility. The same sample was treated under air to oxidize to CuO and under NH_3 to form Cu_3N at 320°C; (B) XRD patterns of samples heated under air and gaseous ammonia. (The peak at 33°C is due to Si 200 forbidden reflection of Si(100) substrate)

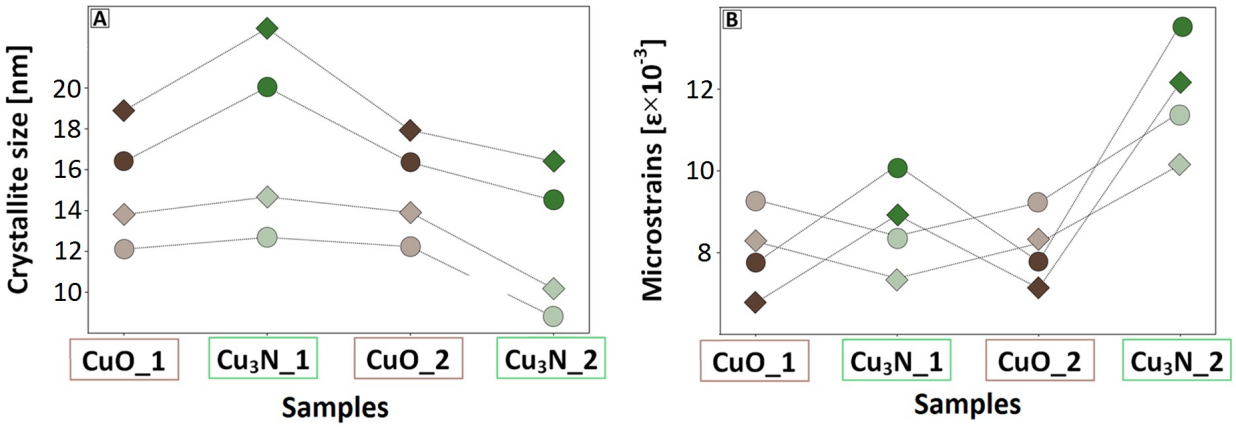

Fig. 4. Changes in (A) crystallite size; (B) microstrains for four samples in the copper oxide (brown) – copper nitride (green) transformation calculated using the full width at half maximum (rhombuses) and the integral breadth (circles) methods. Two peaks for each crystal phase were analyzed: 35 (dark brown) and 38° (light brown) for CuO and 23 (dark green) and 40° (light green) for Cu_3N. The lack of data for the fifth sample – CuO_1 is due to its destruction before measurement

atmospheric conditions, making it difficult to find experiments analogous to ours. Nevertheless, the air or ammonia atmosphere surrounding the heated powder is a key factor affecting crystallite size and microstrain [55–57]. SEM analysis, shown in Fig. 5, was used to investigate the morphology of all samples. The resulting magnifications for copper(II) oxides were 200k× and 500k×, whereas for copper nitrides, only 500k×was obtained. It was observed that in both cases, the materials form separate irregular clusters of nanocrystals. For both **CuO** magnifications, it is possible to see grains that take the form of spherical agglomerates upon annealing. In the case of **Cu_3N**, flat-surfaced grains can be seen, on which scales appear after annealing. The detailed analysis of the size and morphology of the synthesized powders clearly indicates the formation of distinct, sharp-edged grains during successive heat treatments. Initial CuO powder consists of elongated grains with an average length of 80 nm and a width of 40 nm, forming clusters of several hundred nanometers (Figs. 5A, 5F). The first conversion to copper nitride resulted in undefined shapes, appearing as fairly flat clusters of 150–300 nm in size (Fig. 5B). The second thermal transformation conducted in an air atmosphere led to further morphological changes. In this case, measurable 30 nm crystallites grouped into clusters with a width of *ca.* 100 nm and a length of *ca.* 200 nm were visible in SEM images (Figs. 5C, 5G). After the second heating of the powder under an ammonia atmosphere, the nitride powder appears more morphologically defined than **Cu_3N_1**. The clusters visible in Fig. 5D are composed of grains. A rough estimate indicates that these grains are less than 50 nm in size. The next transformation led to the fabrication of copper(II) oxide powder with relatively well-separated grains with visible individual walls. The grain size was about 50 nm (Figs. 5E, 5H). The **CuO_3** SEM images appear with

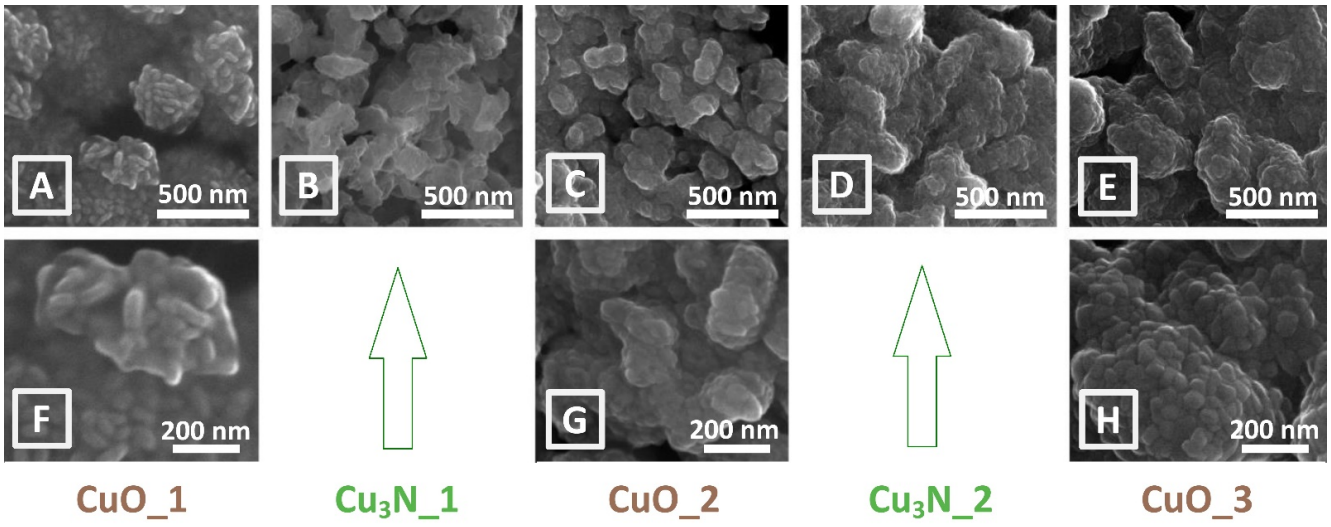

Fig. 5. SEM (SE mode) images of samples heated in air and ammonia. Each column represents samples from left: CuO_1 (images A and F), Cu_3N_1 (image B), CuO_2 (images C and G), Cu_3N_2 (image D) and CuO_3 (images E and H). Images from the top row were obtained at 200k× magnification and from the bottom at 500k×. The lack of high-magnification images for nitrides is due to their poor quality

well-defined edges and shapes, suggesting higher crystallinity, while the more rounded morphology of **CuO_1** may be due to its more amorphous nature. A similar tendency was observed for nitride powders. The explanation for this phenomenon, apart from the increase in crystallinity, may also be the gradual removal of possible amorphous impurities by successive heat treatments.

4. DISCUSSION AND CONCLUSIONS

The present study demonstrates the applicability of using copper(II) nitrate as a precursor for the fabrication of copper nitride powders *via* a gas–solid ammonolysis process. This transformation pathway was thoroughly investigated using *in situ* infrared spectroscopy, X-ray powder diffraction, and scanning electron microscopy, providing a comprehensive tracking of the compositional and morphological changes during the conducted reactions. Copper(II) nitrate is shown to be a convenient and direct precursor for Cu_3N synthesis. The study confirms that this salt undergoes a well-defined transformation pathway through intermediate copper oxides (CuO and Cu_2O) before Cu_3N formation. The Cu–N bond is observed at 320°C, which makes $Cu(NO_3)_2$ a practical and controllable starting material for Cu_3N powder fabrication. Moreover, we presented reversible Cu_3N-CuO transformation under alternating ammonia and air atmospheres, showing significant crystallite size changes in the $NH_{3(g)}$ environment. These features are valuable for applications requiring cycling stability, such as in sensors, catalysts, or battery electrodes.

Presented thermal processing enables the formation of the Cu_3N nanocrystals, with a dripped and dried salt solution as a starting material. The estimated size of the copper nitride fabricated nanocrystals was less than 20 nm. The crystallite size determined from XRD is smaller than the grain size visible in the microscopic images. Most probably, SEM shows grains that contain multiple crystallites. According to the literature, copper oxides, fluorides, and hydroxides can be precursors for this reaction. On the other hand, $Cu_2(OH)_3Cl$ cannot be utilized as a direct precursor for the Cu_3N synthesis [25]. This article indicates that $Cu(NO_3)_2$ can also be considered for this purpose [58,59]. A gas-solid ammonolysis process was also applied by taking as direct precursor other copper salts, including CuF_2 [60], $Cu(CF_3COO)_2$ [26], $Cu(Piv)_2$ (Piv – pivalate) [58], and $CuSiO_3$ [59]. Li *et al.* compared two different precursors to prepare the nitride powder: copper(II) fluoride and copper(II) pivalate ($Cu(OPiv)_2$). Ammonolysis of CuF_2 was performed at 300°C for 8 h, forming large, dense particles with a refined crystallite size of 412 ± 11 nm. In contrast, the ammonolysis of the $Cu(OPiv)_2$ precursor was studied at various temperatures from 180–300°C, and Cu_3N nanoparticles of ~ 20 nm diameter were obtained by heating at 250°C for 10 h, which is close to the values presented by us.

Compared to other nitridation methods, the use of gaseous NH_3 is a simple, effective, and scalable approach. Copper(II) nitrate is non-toxic and commercially available, making it suited for green chemistry and industrial-scale synthesis. Although many recent studies focus on solution-based nitridation (e.g., long-chain amines-assisted), this work underscores the renewed relevance of the historically first ammonolysis method using gaseous NH_3. The ability to control the phase composition, crystallinity, and morphology through simple thermal treatments in adjustable atmospheres – without using high-pressure and high-temperature processing – makes this approach attractive for the tailored synthesis of Cu_3N-based materials.

REFERENCES

[1] P. Paredes, E. Rauwel, and P. Rauwel, "Surveying the Synthesis, Optical Properties and Photocatalytic Activity of Cu_3N Nanomaterials," *Nanomaterials*, vol. 12, no. 13, p. 2218, 2022, doi: 10.3390/nano12132218.

[2] A. Ścigała, E. Szłyk, L. Dobrzańska, D.H. Gregory, and R. Szczęsny, "From binary to multinary copper based nitrides – Unlocking the potential of new applications," *Coord. Chem. Rev.*, vol. 436, p. 213791, 2021, doi: 10.1016/j.ccr.2021.213791.

[3] A. Jiang, M. Qi, and J. Xiao, "Preparation, structure, properties, and application of copper nitride (Cu_3N) thin films: A review," *J. Mater. Sci. Technol.*, vol. 34, no. 9, pp. 1467–1473, 2018, doi: 10.1016/j.jmst.2018.02.025.

[4] M.I. Rodríguez-Tapiador, J.M. Asensi, M. Roldán, J. Merino, J. Bertomeu, and S. Fernández, "Copper Nitride: A Versatile Semiconductor with Great Potential for Next-Generation Photovoltaics," *Coatings*, vol. 13, no. 6, p. 1094, 2023, doi: 10.3390/coatings13061094.

[5] A. Zakutayev *et al.*, "Defect Tolerant Semiconductors for Solar Energy Conversion," *J. Phys. Chem. Lett.*, vol. 5, no. 7, pp. 1117–1125, 2014, doi: 10.1021/jz5001787.

[6] E. Márquez *et al.*, "Optical Properties of Reactive RF Magnetron Sputtered Polycrystalline Cu_3N Thin Films Determined by UV/Visible/NIR Spectroscopic Ellipsometry: An Eco-Friendly Solar Light Absorber," *Coatings*, vol. 13, no. 7, p. 1148, 2023, doi: 10.3390/coatings13071148.

[7] Z. Ji, Y. Zhang, Y. Yuan, and C. Wang, "Reactive DC magnetron deposition of copper nitride films for write-once optical recording," *Mater. Lett.*, vol. 60, no. 29–30, pp. 3758–3760, 2006, doi: 10.1016/j.matlet.2006.03.107.

[8] C. Navío, J. Alvarez, M.J. Capitan, J. Camarero, and R. Miranda, "Thermal stability of Cu and Fe nitrides and their applications for writing locally spin valves," *Appl. Phys. Lett.*, vol. 94, no. 26, p. 263112, 2009, doi: 10.1063/1.3159630.

[9] J. Wang *et al.*, "Cu_3N and its analogs: a new class of electrodes for lithium ion batteries," *J. Mater. Chem. A*, vol. 5, no. 18, pp. 8762–8768, 2017, doi: 10.1039/C7TA02339A.

[10] D. Lee *et al.*, "Copper Nitride Nanowires Printed Li with Stable Cycling for Li Metal Batteries in Carbonate Electrolytes," *Adv. Mater.*, vol. 32, no. 7, p. 1905573, 2020, doi: 10.1002/adma.201905573.

[11] Z.-Q. Liang *et al.*, "Copper-on-nitride enhances the stable electrosynthesis of multi-carbon products from CO_2," *Nat. Commun.*, vol. 9, no. 1, p. 3828, 2018, doi: 10.1038/s41467-018-06311-0.

[12] Z. Yin *et al.*, "Cu_3N Nanocubes for Selective Electrochemical Reduction of CO_2 to Ethylene," *Nano Lett.*, vol. 19, no. 12, pp. 8658–8663, 2019, doi: 10.1021/acs.nanolett.9b03324.

[13] H. Wang, X. Bi, Y. Zhao, Z. Yang, Z. Wang, and M. Wu, "Cu_3N nanoparticles with both (100) and (111) facets for enhancing the selectivity and activity of CO_2 electroreduction to ethylene," *New J. Chem.*, vol. 46, no. 26, pp. 12523–12529, 2022, doi: 10.1039/D2NJ02175G.

[14] Z.Q. Liu, W.J. Wang, T.M. Wang, S. Chao, and S.K. Zheng, "Thermal stability of copper nitride films prepared by rf magnetron sputtering," *Thin Solid Films*, vol. 325, no. 1–2, pp. 55–59, 1998, doi: 10.1016/S0040-6090(98)00448-9.

[15] G. Soto, J.A. Dıěaz, and W. De La Cruz, "Copper nitride films produced by reactive pulsed laser deposition," *Mater. Lett.*, vol. 57, no. 26–27, pp. 4130–4133, 2003, doi: 10.1016/S0167-577X(03)00277-5.

[16] R. Juza and H. Hahn, "Über die Kristallstrukturen von Cu_3N, GaN und InN Metallamide und Metallnitride," *Z. Anorg. Allg. Chem.*, vol. 239, no. 3, pp. 282–287, 1938, doi: 10.1002/zaac.19382390307.

[17] U. Zachwieja and H. Jacobs, "Ammonothermalsynthese von kupfernitrid, Cu_3N," *J. Less-Common Met.*, vol. 161, no. 1, pp. 175–184, 1990, doi: 10.1016/0022-5088(90)90327-G.

[18] J. Choi and E.G. Gillan, "Solvothermal Synthesis of Nanocrystalline Copper Nitride from an Energetically Unstable Copper Azide Precursor," *Inorg. Chem.*, vol. 44, no. 21, pp. 7385–7393, 2005, doi: 10.1021/ic050497j.

[19] P. Xi *et al.*, "Solvothermal synthesis of magnetic copper nitride nanocubes with highly electrocatalytic reduction properties," *RSC Adv.*, vol. 4, no. 27, pp. 14206–14209, 2014, doi: 10.1039/C4RA01307G.

[20] H. Wu and W. Chen, "Copper Nitride Nanocubes: Size-Controlled Synthesis and Application as Cathode Catalyst in Alkaline Fuel Cells," *J. Am. Chem. Soc.*, vol. 133, no. 39, pp. 15236–15239, 2011, doi: 10.1021/ja204748u.

[21] R. Deshmukh, G. Zeng, E. Tervoort, M. Staniuk, D. Wood, and M. Niederberger, "Ultrasmall Cu_3N Nanoparticles: Surfactant-Free Solution-Phase Synthesis, Nitridation Mechanism, and Application for Lithium Storage," *Chem. Mater.*, vol. 27, no. 24, pp. 8282–8288, 2015, doi: 10.1021/acs.chemmater.5b03444.

[22] S. Mondal and C.R. Raj, "Copper Nitride Nanostructure for the Electrocatalytic Reduction of Oxygen: Kinetics and Reaction Pathway," *J. Phys. Chem. C*, vol. 122, no. 32, pp. 18468–18475, 2018, doi: 10.1021/acs.jpcc.8b03840.

[23] T. Nakamura, H. Hayashi, and T. Ebina, "Preparation of copper nitride nanoparticles using urea as a nitrogen source in a long-chain alcohol," *J. Nanopart. Res.*, vol. 16, no. 11, p. 2699, 2014, doi: 10.1007/s11051-014-2699-1.

[24] A. Scigala *et al.*, "Copper Nitride Nanowire Arrays – Comparison of Synthetic Approaches," *Materials*, vol. 14, no. 3, p. 603, 2021, doi: 10.3390/ma14030603.

[25] R. Szczęsny, T.K. A. Hoang, L. Dobrzańska, and D.H. Gregory, "Solution/Ammonolysis Syntheses of Unsupported and Silica-Supported Copper(I) Nitride Nanostructures from Oxidic Precursors," *Molecules*, vol. 26, no. 16, p. 4926, 2021, doi: 10.3390/molecules26164926.

[26] R. Szczęsny, E. Szłyk, M.A. Wiśniewski, T.K. A. Hoang, and D.H. Gregory, "Facile preparation of copper nitride powders and nanostructured films," *J. Mater. Chem. C*, vol. 4, no. 22, pp. 5031–5037, 2016, doi: 10.1039/C6TC00493H.

[27] R. Szczęsny *et al.*, "Low-cost preparation and characterization of new CuO/ZnO and Cu_3N/ZnO nanocomposites," *J. Cryst. Growth*, vol. 651, p. 128004, 2025, doi: 10.1016/j.jcrysgro.2024.128004.

[28] Z. Wang *et al.*, "Copper-Nitride Nanowires Array: An Efficient Dual-Functional Catalyst Electrode for Sensitive and Selective Non-Enzymatic Glucose and Hydrogen Peroxide Sensing," *Chem. A Eur. J.*, vol. 23, no. 21, pp. 4986–4989, 2017, doi: 10.1002/chem.201700366.

[29] J. Zawadzki, M. Wiśniewski, and K. Skowrońska, "Heterogeneous reactions of NO_2 and NO–O_2 on the surface of carbons," *Carbon*, vol. 41, no. 2, pp. 235–246, 2003, doi: 10.1016/S0008-6223(02)00281-6.

[30] J. Zawadzki and M. Wiśniewski, "An infrared study of the behavior of SO_2 and NO_x over carbon and carbon-supported catalysts," *Catal. Today*, vol. 119, no. 1–4, pp. 213–218, 2007, doi: 10.1016/j.cattod.2006.08.037.

[31] M. Wiśniewski, S. Furmaniak, A.P. Terzyk, P.A. Gauden, and P. Kowalczyk, "Properties of Phenol Confined in Realistic Carbon Micropore Model: Experiment and Simulation," *J. Phys. Chem. C*, vol. 119, no. 34, pp. 19987–19995, 2015, doi: 10.1021/acs.jpcc.5b06136.

[32] J. Zawadzki and M. Wiśniewski, "In situ characterization of interaction of ammonia with carbon surface in oxygen atmosphere," *Carbon*, vol. 41, no. 12, pp. 2257–2267, 2003, doi: 10.1016/S0008-6223(03)00251-3.

[33] J. Zawadzki, M. Wiśniewski, J. Weber, O. Heintz, and B. Azambre, "IR study of adsorption and decomposition of propan-2-ol on carbon and carbon-supported catalysts," *Carbon*, vol. 39, no. 2, pp. 187–192, 2001, doi: 10.1016/S0008-6223(00)00107-X.

[34] Y. Zhan, X. Zhou, B. Fu, and Y. Chen, "Catalytic wet peroxide oxidation of azo dye (Direct Blue 15) using solvothermally synthesized copper hydroxide nitrate as catalyst," *J. Hazard. Mater.*, vol. 187, no. 1–3, pp. 348–354, 2011, doi: 10.1016/ j.jhaz mat.2011.01.027.

[35] S. Sun, X. Zhang, Y. Sun, S. Yang, X. Song, and Z. Yang, "Hierarchical CuO nanoflowers: water-required synthesis and their application in a nonenzymatic glucose biosensor," *Phys. Chem. Chem. Phys.*, vol. 15, no. 26, p. 10904, 2013, doi: 10.1039/c3cp50922b.

[36] C. Henrist, K. Traina, C. Hubert, G. Toussaint, A. Rulmont, and R. Cloots, "Study of the morphology of copper hydroxynitrate nanoplatelets obtained by controlled double jet precipitation and urea hydrolysis," *J. Cryst. Growth*, vol. 254, no. 1–2, pp. 176–187, 2003, doi: 10.1016/S0022-0248(03)01145-X.

[37] I.V. Morozov, K.O. Znamenkov, Yu. M. Korenev, and O.A. Shlyakhtin, "Thermal decomposition of $Cu(NO_3)_2$•$3H_2O$ at reduced pressures," *Thermochim. Acta*, vol. 403, no. 2, pp. 173–179, 2003, doi: 10.1016/S0040-6031(03)00057-1.

[38] B.V. L'vov and A.V. Novichikhin, "Mechanism of thermal decomposition of hydrated copper nitrate in vacuo," *Spectrochim. Acta Part B-At. Spectrosc.,* vol. 50, no. 12, pp. 1459–1468, 1995, doi: 10.1016/0584-8547(95)01402-0.

[39] K. Nakamoto, *Infrared and Raman spectra of Inorganic and Coordination Compounds. Part B: Applications in Coordination, Organometallic, and Bioinorganic Chemistry.* New Jersey: Wiley, 2009.

[40] B. Lefez, R. Souchet, K. Kartouni, and M. Lenglet, "Infrared reflection study of CuO in thin oxide films," *Thin Solid Films*, vol. 268, no. 1–2, pp. 45–48, 1995, doi: 10.1016/0040-6090(95)06872-4.

[41] M.S. Alhumaimess, A.A. Essawy, M.M. Kamel, I.H. Alsohaimi, and H.M.A. Hassan, "Biogenic-Mediated Synthesis of Mesoporous Cu_2O/CuO Nano-Architectures of Superior Catalytic Reductive towards Nitroaromatics," *Nanomaterials*, vol. 10, no. 4, p. 781, 2020, doi: 10.3390/nano10040781.

[42] A. Sahai, N. Goswami, S.D. Kaushik, and S. Tripathi, "Cu/Cu_2O/CuO nanoparticles: Novel synthesis by exploding wire technique and extensive characterization," *Appl. Surf. Sci.*, vol. 390, pp. 974–983, 2016, doi: 10.1016/j.apsusc.2016.09.005.

[43] S. Bouachma *et al.*, "Synthesis of PSi-n/CuO-p/Cu_2O-n heterostructure for CO_2 gas sensing at room temperature," *Appl. Phys. A*, vol. 128, no. 1, p. 69, 2022, doi: 10.1007/s00339-021-05167-4.

[44] M. Muthukumaran, S. Niranjani, K.S. Barnabas, V. Narayanan, T. Raju, and K. Venkatachalam, "Green Route Synthesis and Characterization of Cuprous Oxide (Cu_2O): Visible light Irradiation photocatalytic activity of MB Dye," *Mater. Today-Proc.*, vol. 14, pp. 563–568, 2019, doi: 10.1016/j.matpr.2019.04.179.

[45] C. Chen, H. Xu, L. Xu, F. Zhang, J. Dong, and H. Wang, "One-pot synthesis of homogeneous core–shell Cu_2O films with nanoparticle-composed multishells and their photocatalytic properties," *RSC Adv.*, vol. 3, no. 47, p. 25010, 2013, doi: 10.1039/c3ra43450h.

[46] R. Kadzutu-Sithole *et al.*, "Elucidating the effect of precursor decomposition time on the structural and optical properties of copper(ı) nitride nanocubes," *RSC Adv.*, vol. 10, no. 56, pp. 34231–34246, 2020, doi: 10.1039/C9RA09546B.

[47] A.R. Bushroa, R.G. Rahbari, H.H. Masjuki, and M.R. Muhamad, "Approximation of crystallite size and microstrain via XRD line broadening analysis in TiSiN thin films," *Vacuum*, vol. 86, no. 8, pp. 1107–1112, 2012, doi: 10.1016/j.vacuum.2011.10.011.

[48] K. Maniammal, G. Madhu, and V. Biju, ' 'X-ray diffraction line profile analysis of nanostructured nickel oxide: Shape factor and convolution of crystallite size and microstrain contributions," *Phys. E:Low-dimension. Syst. Nanostruct.*, vol. 85, pp. 214–222, 2017, doi: 10.1016/j.physe.2016.08.035.

[49] L.K. Singh, A. Bhadauria, S. Jana, and T. Laha, "Effect of Sintering Temperature and Heating Rate on Crystallite Size, Densification Behaviour and Mechanical Properties of Al-MWCNT Nanocomposite Consolidated via Spark Plasma Sintering," *Acta Metall. Sin. (Engl. Lett.)*, vol. 31, no. 10, pp. 1019–1030, 2018, doi: 10.1007/s40195-018-0795-4.

[50] M. Kurian and C. Kunjachan, "Investigation of size dependency on lattice strain of nanoceria particles synthesised by wet chemical methods," *Int. Nano Lett.*, vol. 4, no. 4, pp. 73–80, 2014, doi: 10.1007/s40089-014-0122-7.

[51] F.A. Akgul, G. Akgul, N. Yildirim, H.E. Unalan, and R. Turan, "Influence of thermal annealing on microstructural, morphological, optical properties and surface electronic structure of copper oxide thin films," *Mater. Chem. Phys.*, vol. 147, no. 3, pp. 987–995, 2014, doi: 10.1016/j.matchemphys.2014.06.047.

[52] M. Khammar, F. Ynineb, S. Guitouni, Y. Bouznit, and N. Attaf, "Crystallite size and intrinsic strain contribution in band gap energy redshift of ultrasonic-sprayed kesterite CZTS nanostructured thin films," *Appl. Phys. A*, vol. 126, no. 6, p. 398, 2020, doi: 10.1007/s00339-020-03591-6.

[53] S.J. Henderson and A.L. Hector, "Structural and compositional variations in Ta_3N_5 produced by high-temperature ammonolysis of tantalum oxide," *J. Solid State Chem.*, vol. 179, no. 11, pp. 3518–3524, 2006, doi: 10.1016/j.jssc.2006.07.021.

[54] S. Yoon *et al.*, "The Influence of the Ammonolysis Temperature on the Photocatalytic Activity of β-TaON," *Int. J. Photoenergy*, vol. 2013, pp. 1–8, 2013, doi: 10.1155/2013/507194.

[55] Ř. Borg *et al.*, "Effect of calcination atmosphere and temperature on γ-Al_2O_3 supported cobalt Fischer-Tropsch catalysts," *Top Catal.*, vol. 45, no. 1–4, pp. 39–43, 2007, doi: 10.1007/s11244-007-0237-4.

[56] H. Slimen, H. Lachheb, S. Qourzal, A. Assabbane, and A. Houas, "The effect of calcination atmosphere on the structure and photoactivity of TiO_2 synthesized through an unconventional doping using activated carbon," *J. Environ. Chem. Eng.*, vol. 3, no. 2, pp. 922–929, 2015, doi: 10.1016/j.jece.2015.02.017.

[57] O. Kikhtyanin, V. Pospelova, J. Aubrecht, M. Lhotka, and D. Kubička, "Effect of Calcination Atmosphere and Temperature on the Hydrogenolysis Activity and Selectivity of Copper-Zinc Catalysts," *Catalysts*, vol. 8, no. 10, p. 446, 2018, doi: 10.3390/catal8100446.

[58] X. Li, A.L. Hector, and J.R. Owen, "Evaluation of Cu_3N and CuO as Negative Electrode Materials for Sodium Batteries," *J. Phys. Chem. C*, vol. 118, no. 51, pp. 29568–29573, 2014, doi: 10.1021/jp509385w.

[59] R. Deshmukh and U. Schubert, "Synthesis of CuO and Cu_3N Nanoparticles in and on Hollow Silica Spheres," *Eur. J. Inorg. Chem.*, vol. 2013, no. 14, pp. 2498–2504, 2013, doi: 10.1002/ejic.201201442.

[60] G. Paniconi, Z. Stoeva, H. Doberstein, R.I. Smith, B.L. Gallagher, and D.H. Gregory, "Structural chemistry of Cu_3N powders obtained by ammonolysis reactions," *Solid State Sci.*, vol. 9, no. 10, pp. 907–913, 2007, doi: 10.1016/j.solidstatesciences.2007.03.017.